Cross polarization in swept beam THz imaging systems using off-axis parabolic mirrors

Rezapoor, Pouyan; Tamminen, Aleksi ; Tamminen, Aleksi ; Ala-Laurinaho, Juha; Llombart, Nuria; Rodilla, Helena ; Stake, Jan; Taylor, Zachary D.

DOI
10.23919/EuCAP53622.2022.9769500

Publication date
2022

Document Version
Final published version

Published in
2022 16th European Conference on Antennas and Propagation (EuCAP)

Cross polarization in swept beam THz imaging systems using off-axis parabolic mirrors

Pouyan Rezapoor*, Aleksi Tamminen*, Irina Nefedova*, Juha Ala-Laurinaho*, Nuria Llombart ‡, Helena Rodilla†, Jan Stake†, Zachary Taylor*
*Department of Electronics and Nanoengineering, Aalto University, Espoo, Finland, pouyan.rezapoor@aalto.fi
†Chalmers University of Technology, Gothenburg, Sweden
‡Delft University of Technology, Delft, Netherlands

***Abstract*—The optical behavior of a terahertz imaging system employing a train of four identical off-axis parabolic mirrors with oblique incidence angle illumination is investigated in this work. The aperture filling and aberrations of a single off-axis parabolic mirror when illuminated by a Gaussian terahertz beam at its focus point is measured and simulated. The amplitude of E-field in transverse electric (TE) and transverse magnetic (TM) polarizations at target plane reveals a significant cross polarization, even when there is zero cross polarization at the source beam, amplitude of which is $\sim 33\%$ of TE polarization. The investigation of the E-field on the detector plane reveals that this ratio is $\sim 1.5\%$ at the detector plane, and the cross polarized E-field at the target plane is rotated back to co polarization. Although its amplitude is negligible, the TM distribution at detector plane is bimodal and tilted about the optical axis.**

***Index Terms*—THz, sub-millimeter wave, polarization, off-axis parabolic mirror.**

I. Introduction

The majority of THz medical imaging systems for *in-vivo* applications are active modalities with single source, single detector designs. These reflective THz systems also typically utilize THz time domain spectroscopy (TDS) and THz time domain imaging with separate source detector in their own apertures. Optical co-location via beamsplitters is possible although dynamic range drops by at least 6 dB and it is difficult to realize robust quasi-optical beamsplitters that can operate over > 1 decade of bandwidth. Optical circulator technology for a shared source detector aperture is now coming on line but has not yet achieved significant adoption. The consequence of these challenges is oblique illumination.

Broad bandwidth and limited power budget inherent to THz spectroscopic imaging systems make quasi-optical component absorption and dispersion mitigation a high priority. To this end, most systems use off-axis parabolic (OAP) or off-axis elliptical (OAE) mirrors for beam collimation and focusing. Also, partly a consequence of bandwidth, the majority of sources and detectors are linearly polarized due to antenna choices and/or TE transmission lines feeding the device antenna.

The resulting system phenomenology is reflective imaging system that optically couples a separate source and detector through a train of aspheric mirrors with oblique illumination. The mirror train is often composed of identical mirror pairs which are rotated, with respect to each other, about one of their axes to a certain angle to map the source axis to the sample plane axis and then sample plane axis back to the detector axis. Aspheric mirror pairs that are not oriented mirror symmetric are known to generate significant cross polarization [1], [2]. In this paper, TE and TM are considered E-field components along Y- and Z-axis, respectively, as illustrated later in Fig. 3.

On the application side, *in vivo* THz measurements of skin usually require flattening the sample with a dielectric window of quartz or a low-loss polymer to create a specular reflection whose spectral properties are due to bulk tissue permittivity variation and not geometry. The reflection coefficients at the air-window and window-tissue interfaces are polarization dependent. Deconvolution of window etalon from tissue properties is performed via Fresnel equations. Successful deconvolution requires precise knowledge and/or control of illumination polarization [3].

In vivo THz measurements of skin require a window [4] and assume illumination polarization is linear and also co-linear with either target TE or TM. Due to significant generation of cross polarization at the target plane, as discussed in this paper, this is likely not realizable. This paper reports on significant cross polarization at the target plane generated by standard OAP mirror pairs coupled to a linearly polarized source. The analysis shows the subsequent OAP mirror pair rotates target TM back to TE at the detector plane. A canonical, four-OAP system is presented and physical-optics simulation of Gaussian beams at 330, 415, and 500 GHz are conducted. The beams are routed from the source plane and coupled to a detector with the same beam pattern as the source. Beam profiles and polarization are checked at the relevant planes. Preliminary planar near-field scanning measurements of the beam after collimation by an OAP mirror are also presented to check the applicability of the simulations.

II. Optical System & Implementation

An example of skin tissue model under illumination of TE and TM field is illustrated in Fig. 1. The hydration profile of the tissue is assumed to be linear in stratum corneum and epidemis, and constant in the dermis [5]. Polarization and incidence angle dependence of the skin tissue reflection magnitude is shown in Fig. 2. Tissue permittivity was computed with Bruggeman effective media theory [6], [7] (two component mixture) using the double Debye model for water [8], [9] and

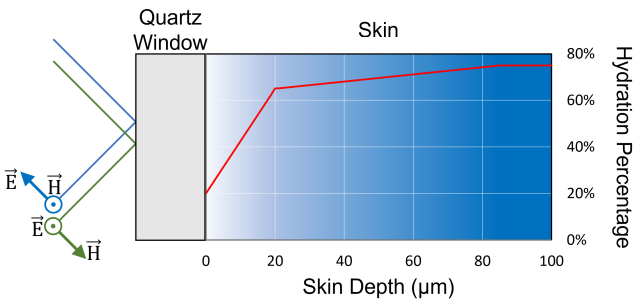

Fig. 1. TE (green) and TM (blue) fields incident on skin with quartz window. water concentration profile is approximately linear in the stratum corneum ($20\mu m$) and epidermal region ($20-85\mu m$), and constant in the dermal reservoir. Skin surface, epidermis, and dermis hydration percentages are assumed to be 20%, 65%, and 75%, respectively.

$\epsilon_r = 2.9$ for the non-aqueous tissue constituent. The water volume fraction was according to Fig. 1. Fresnel equations were used to compute the reflection coefficient at the interface using quartz crystal window and illumination angles of 19°, 30°, and 45°, and mapping these to interface angle via Snell's laws and a dispersion free quartz permittivity of $\epsilon_r = 4$. The TE polarization reflectivity is plotted in a solid line style and TM in the dotted line style. Overall, we can see that the reflectivity depends on illumination angle and polarization. Thus, if a measurement is some unknown weighted average of TE and TM target incidence, the level of the reflevtivity to a single polarization will result in substantial error in estimated permittivity and thus water content.

An example of a THz imaging system with oblique incidence angle illumination employing a train of four identical OAP mirrors is illustrated in Fig. 3. THz beam source is located at focus point of the OAP mirror M1. After being collimated by M1, it is focused on the target plane by M2,

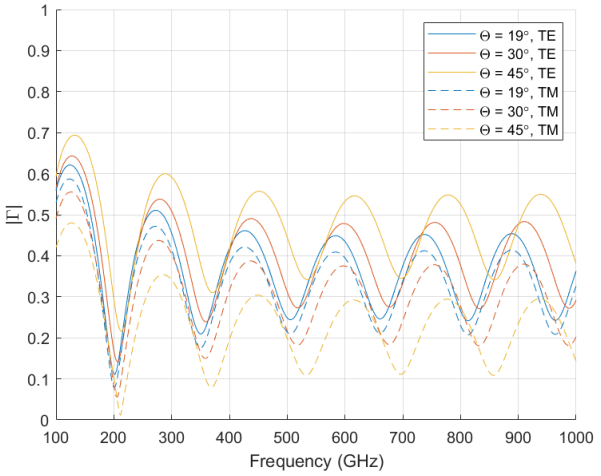

Fig. 2. Dependence of skin reflection magnitude on polarization and incidence angle.

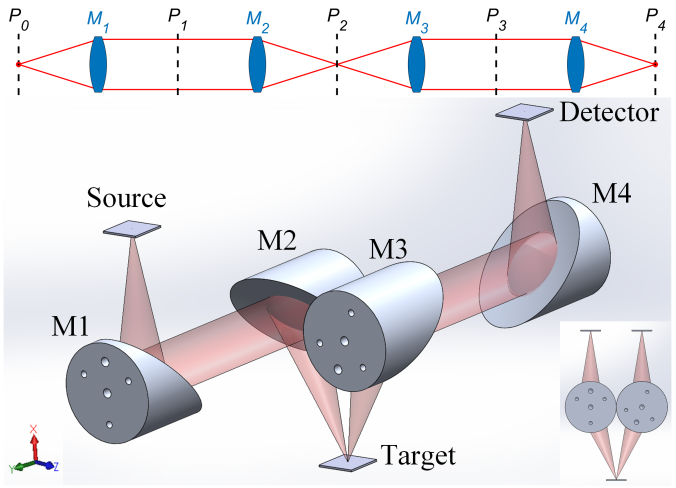

Fig. 3. THz imaging system with oblique incidence angle illumination employing a train of four identical OAPs.

and the reflected beam is collected and focused at the detector plane by M3 & M4. In order to minimize errors, OAP mirrors are all identical, with $\theta = 90°$, effective focal length of $f_e = 76.2$ mm, and clear aperture diameter of $D = 50.8$ mm. The distance between mirrors M1 & M2 and between mirrors M3 & M4 are equal to $1.3f_e = 101.6$ mm, and the setup is symmetric. P_0-P_4 show the locations of the observation planes in physical-optics simulations with respect to the optical path.

In order to maximize the confocality of the quasi-optical design illustrated in Fig. 3, the aperture of the first mirror M1 needs to be filled with acceptable edge taper. Thus, the collimated beam propagated from an OAP mirror needs to be measured and simulated. For this purpose, we assume a setup where the OAP is illuminated by a THz Gaussian-beam waist at the focus and the beam propagation is measured by a detector at a distance from its center and along its optical axis (in plane P_1). The distance between the detector and the OAP is taken to be equal to the distance between M1 and M2 in the

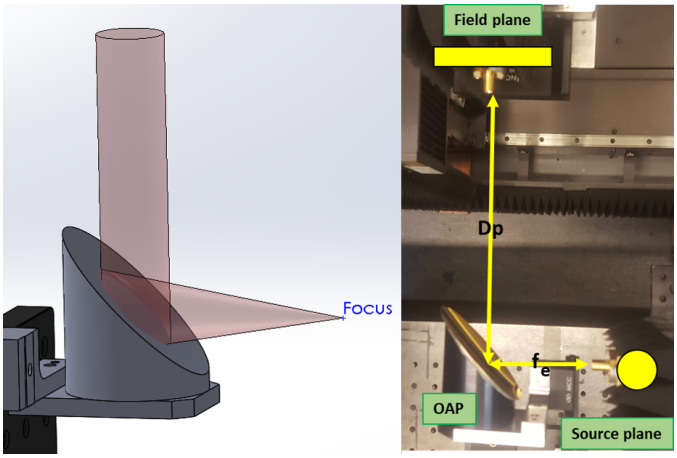

Fig. 4. Experimental setup for OAP mirror measurements. Mirror specifications are: $D = 50.8$ mm, $f_e = 76.2$ mm, & $\theta = 90°$.

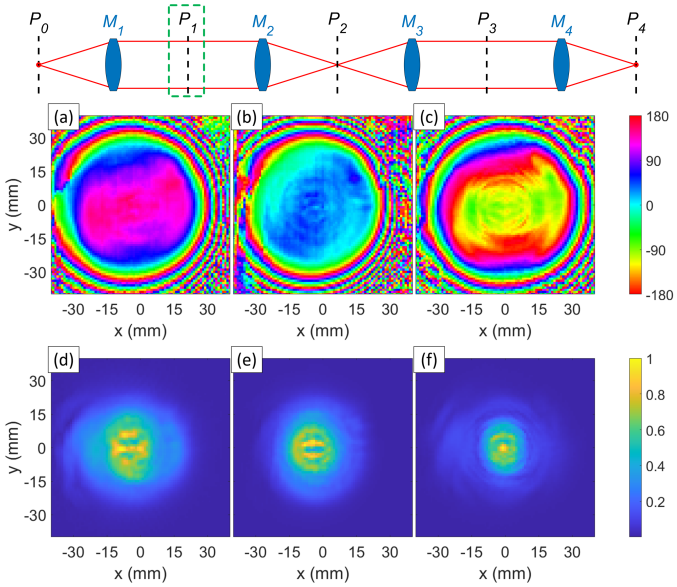

Fig. 5. Measured (a,b,c) phase and (d,e,f) magnitude of the scattering parameter S_{21} for a single OAP reflector at (a,d) 330 GHz, (b,e) 415 GHz, and (c,f) 500 GHz.

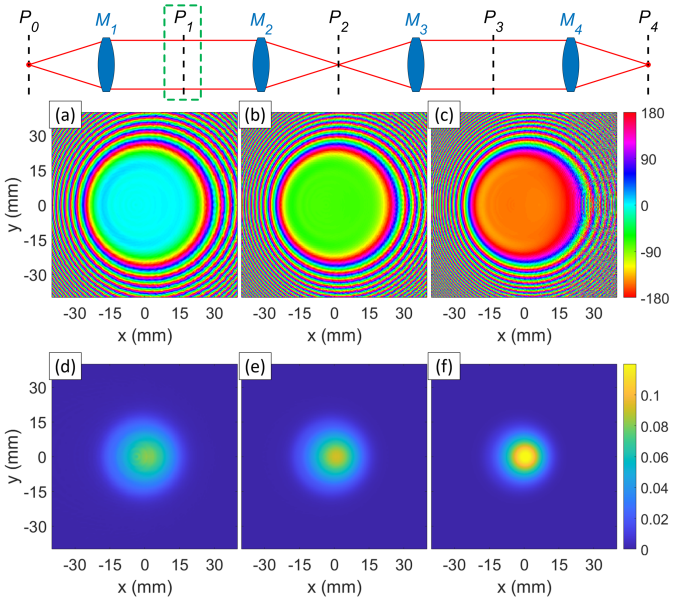

Fig. 6. Simulated (a,b,c) phase and (d,e,f) magnitude of the TE field for a single OAP reflector at (a,d) 330 GHz, (b,e) 415 GHz, and (c,f) 500 GHz.

setup illustrated in Fig. 3. Related experimental setup is shown in Fig. 4. The source is a Gaussian beam illuminated by a WR-2.2 frequency extender, with the frequency range 325 GHz – 500 GHz, coupled to a Pickett-Potter horn antenna. With a near-field scanner, another frequency extender scans the field plane and both detectors are connected to a vector-network analyzer (VNA). The scattering parameter S_{21}, measured by the VNA mostly along TE polarization with open-ended waveguide as probe, results in the beam propagation at the detector plane P_1.

III. Results

A. Single OAP mirror measurement

The magnitude and phase of the measured scattering parameter S_{21} in the plane P_1 is presented in Fig. 5 for the input frequency of 330 GHz, 415 GHz, and 500 GHz. The amplitude of the collimated beam is Gaussian with a frequency dependence, and its phase shows that the beam fills the mirror aperture with small aberrations, independent of the frequency. These small aberrations arise from the tolerances in implementation and the fact that the phase center location relative to horn aperture has a variation vs. frequency in both E-planes and H-planes. The measured data illustrated in Fig. 5 suggest that the aperture of the OAP is filled with the source Gaussian beam and a planar phase along the mirror's aperture plane is detected.

Next, the physical-optics simulations of the setup (Fig. 4) are presented with comparison to the measurements. Fig. 6 shows the TE field magnitude and phase at the detector plane P_1 in physical-optics simulations of this setup, which agree with the experimental results. The input in the physical-optics simulations is a Gaussian beam that was fit to the Pickett-Potter horn parameters to match the results with the experiment. An expected asymmetry about the aperture centroid is also visible, since the mirror is off-axis. The edge taper (defined as the ratio of the E-field magnitude at the edge of the mirror to the maximum E-field magnitude on the mirror surface) in these cases are -12.43 dB, -18.13 dB, and -30.34 dB at 330 GHz, 415 GHz, and 500 GHz, respectively, suggesting that the beam collimation is achieved with acceptable edge effects. The simulation results are close to the experiment. In practice, the output of a Pickett-Potter horn is not a pure Gaussian beam, as assumed in the simulations, and its phase center has a variation as a function of the frequency, which adds tolerance to precise positioning of the source beam in focus point of the OAP mirror.

B. Generation of cross polarization

According to the rotation of M2 & M3 in Fig. 3 to achieve oblique incidence angle, we expect some cross polarization to be generated at the target plane. This means that, by assuming TE polarization along the optical axis of the mirrors (Y-axis) and TM polarization along the rotation plane of M2 & M3 (Z-axis), there will be significant E-field magnitude along the TM polarization. Physical-optics simulations prove this point and suggest that significant knowledge of the E-field polarization should also be taken into account in Fresnel equations to deconvolve tissue properties from the window.

Fig. 7 shows the magnitude of the E-field on the target plane P_2 (which is also expected to be Gaussian) along TE and TM polarizations, with the TE and TM polarizations spatially collocated. TM field amplitude is $\sim 33\%$ of TE, suggesting that the intrinsic contrast produced by TM polarization is not negligible in comparison with TE polarization, and we cannot assume one polarization state (i.e., TE) at the interface between air and the target.

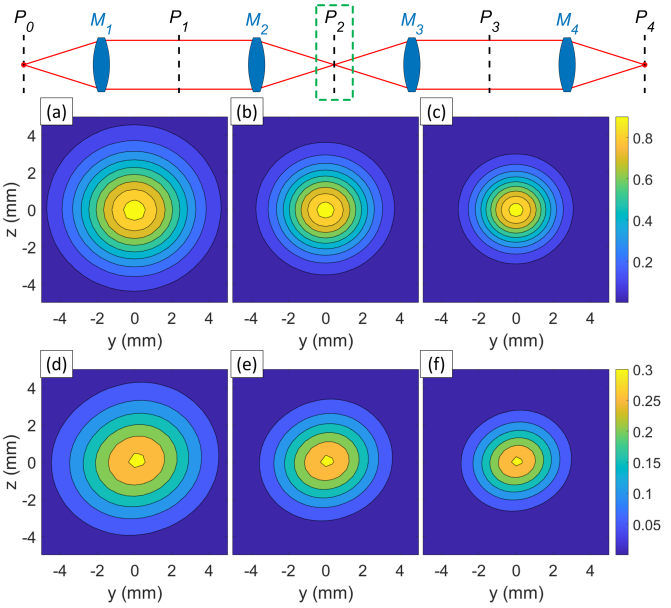

Fig. 7. (a,b,c) Y-component and (d,e,f) Z-component of the simulated E-field magnitude on the target plane in the THz imaging system at (a,d) 330 GHz, (b,e) 415 GHz, and (c,f) 500 GHz.

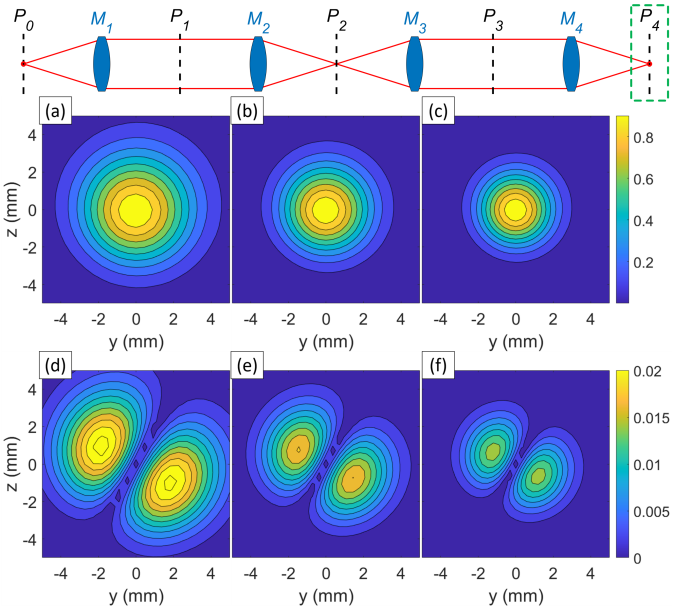

Fig. 8. (a,b,c) TE and (d,e,f) TM simulated magnitude of the E-field on the detector plane in the THz imaging system at (a,d) 330 GHz, (b,e) 415 GHz, and (c,f) 500 GHz.

C. Field at the detector plane

Physical-optics simulations of the E-field magnitude in TE and TM polarizations at the detector plane P_4 reveal that TM amplitude is $\sim 1.5\%$ of TE at WR-2.2 midband frequency (415 GHz). Since this ratio was $\sim 33\%$ in the target plane, we can conclude that TM in the target plane has been rotated back to TE in the detector plane, mainly because of the structure's symmetry.

Fig. 8 shows the physical-optics simulation results for the E-field magnitude on the detector plane in TE and TM polarization, when the target plane is located at the focal plane of the mirrors M2 & M3. These results reveal that, although it has a very small magnitude, the TM distribution at the detector plane is bimodal and tilted about the optical axis.

IV. Conclusion

THz medical imaging has been recently applied with oblique incidence angle illumination, using OAP mirrors. Most medical imaging system research sandwiches or flattens tissue against single crystal or sapphire windows, and deconvolution of window etalon from tissue properties is performed via Fresnel equations, and usually TDS and frequency domain systems utilize linearly polarized antennas and thus assume one polarization state in the air crystal interface.

This work has shown that there is significant TM polarization generated at the target interface, eventhough the source is purely TE polarized, and TM magnitude is $\sim 33\%$ of TE. It is also shown that the reflected TM is rotated back to TE at the detector plane due to structure's symmetry and the E-field magnitude in TM polarization is $\sim 1.5\%$ of the TE polarization at WR-2.2 midband frequency (415 GHz). One suggestion to reduce target cross polarization is to use OAP mirrors with smaller off-set angle.

References

[1] S. Ghobrial, "Off-axis cross-polarization and polarization efficiencies of reflector antennas," *IEEE Transactions on Antennas and Propagation*, vol. 27, no. 4, pp. 460–466, 1979.

[2] Z. D. Taylor, S. Sung, J. Garritano, N. Bajwa, B. Nowroozi, N. Llombart, P. Tewari, and W. S. Grundfest, "Optical design for translation of thz medical imaging technology," in *Terahertz, RF, Millimeter, and Submillimeter-Wave Technology and Applications VII*, vol. 8985. International Society for Optics and Photonics, 2014, p. 89850H.

[3] Z. D. Taylor, R. S. Singh, D. B. Bennett, P. Tewari, C. P. Kealey, N. Bajwa, M. O. Culjat, A. Stojadinovic, H. Lee, J.-P. Hubschman *et al.*, "Thz medical imaging: in vivo hydration sensing," *IEEE transactions on terahertz science and technology*, vol. 1, no. 1, pp. 201–219, 2011.

[4] Q. Sun, R. I. Stantchev, J. Wang, E. P. Parrott, A. Cottenden, T.-W. Chiu, A. T. Ahuja, and E. Pickwell-MacPherson, "In vivo estimation of water diffusivity in occluded human skin using terahertz reflection spectroscopy," *Journal of biophotonics*, vol. 12, no. 2, p. e201800145, 2019.

[5] D. B. Bennett, W. Li, Z. D. Taylor, W. S. Grundfest, and E. R. Brown, "Stratified media model for terahertz reflectometry of the skin," *IEEE Sensors Journal*, vol. 11, no. 5, pp. 1253–1262, 2010.

[6] G. A. Niklasson, C. Granqvist, and O. Hunderi, "Effective medium models for the optical properties of inhomogeneous materials," *Applied Optics*, vol. 20, no. 1, pp. 26–30, 1981.

[7] K. K. Karkkainen, A. H. Sihvola, and K. I. Nikoskinen, "Effective permittivity of mixtures: numerical validation by the fdtd method," *IEEE Transactions on Geoscience and Remote Sensing*, vol. 38, no. 3, pp. 1303–1308, 2000.

[8] J. Xu, K. W. Plaxco, S. J. Allen, J. E. Bjarnason, and E. R. Brown, "0.15–3.72 thz absorption of aqueous salts and saline solutions," *Applied physics letters*, vol. 90, no. 3, p. 031908, 2007.

[9] H. J. Liebe, G. A. Hufford, and T. Manabe, "A model for the complex permittivity of water at frequencies below 1 thz," *International Journal of Infrared and Millimeter Waves*, vol. 12, no. 7, pp. 659–675, 1991.